ORGANOMETALLICS

Article

pubs.acs.org/Organometallics

Mechanistic Insights into Concerted C−C Reductive Elimination from Homoleptic Uranium Alkyls

Sara A. Johnson,[†] Robert F. Higgins,[‡] Mahdi M. Abu-Omar,[†] Matthew P. Shores,[‡] and Suzanne C. Bart*[,†]

[†]H.C. Brown Laboratory, Department of Chemistry, Purdue University, West Lafayette, Indiana 47906, United States

[‡]Department of Chemistry, Colorado State University, Ft. Collins, Colorado 80523, United States

Supporting Information

ABSTRACT: A mechanistic study was carried out to probe concerted C−C reductive elimination from homoleptic uranium(IV) alkyls. The *para*-chloro uranium(IV) tetrabenzyl derivative, $U(CH_2-p\text{-}ClC_6H_4)_4$ (**2-*p*-Cl**), was synthesized by treating UCl_4 with 4 equivalents of KCH_2-p-Cl-Ph (**1-*p*-Cl**) at −108 °C, adding a new member to the previously reported family of uranium alkyl complexes $U(CH_2C_6H_5)_4$ (**2-Bn**), $U(CH_2-p\text{-}^iPrC_6H_4)_4$ (**2-*p*-^{i}Pr**), $U(CH_2-p^tBu\text{-}C_6H_4)_4$ (**2-*p*-^{t}Bu**), $U(CH_2-o\text{-}OMeC_6H_4)_4$ (**2-*o*-OMe**), and $U(CH_2-m\text{-}OMeC_6H_4)_4$ (**2-*m*-OMe**). Each member of this family readily reacts with the redox-active α-diimine ligand, $^{Mes}DAB^{Me}$ ($^{Mes}DAB^{Me}$ = [MesN═C(Me)C(Me)═NMes]; Mes = 2,4,6-trimethylphenyl), to afford the products from C−C reductive elimination, namely, $(^{Mes}DAB^{Me})U(CH_2Ph')_2$ and $Ph'CH_2CH_2Ph'$ (Ph′ = p-^{i}PrC$_6$H$_4$, p-^{t}BuC$_6$H$_4$, m-OMeC$_6$H$_4$, p-ClC$_6$H$_4$). Room-temperature magnetic-susceptibility values, obtained via SQUID magnetometry, show a correlation with an increase in the magnetic moment as the electron-withdrawing character of the substituent increases. Kinetic studies were used to assess the effect of the benzyl substituent on the rate of reductive elimination, showing that reaction rate increases as the electron-withdrawing nature of the substitution increases. Eyring data revealed a large and negative entropy value, indicative of a highly ordered transition state, consistent with the previously reported concerted elimination concluded from crossover experiments.

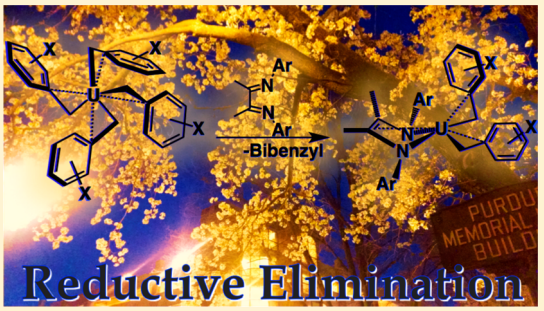

INTRODUCTION

As a key fundamental organometallic reaction, carbon−carbon reductive elimination has been studied widely for its synthetic applications and mechanistic details.[1−10] This process is well understood for transition metals, especially late precious metals, but relatively little is known about such an important bond-forming step for the actinide elements. This is in part due to (1) the multielectron step requirement for reductive elimination, which is not characteristic of the actinide elements and (2) the paucity of organoactinide compounds with two or more labile alkyls as compared to transition-metal organometallic complexes.[11]

In 2012, we reported the isolation of the first neutral, homoleptic uranium(IV) alkyl, tetrabenzyluranium.[12] While its group IV (Ti, Zr, Hf)[13−15] and thorium[16] counterparts had been known for decades, the uranium analogue had remained elusive. The generation of $U(CH_2Ph)_4$ (**2-Bn**) was significant, as it provided a platform to study carbon−carbon bond formation via reductive elimination at uranium(IV). Such a process would normally lead to an unstable uranium(II) bis(benzyl) product, but utilization of a redox-active α-diimine ligand circumvented this problem by storing two electrons gained from the reductive elimination reaction (eq 1). Thus, the organometallic product, $(^{Mes}DAB^{Me})U(CH_2C_6H_5)_2$ (**3-Bn**) featured a ligand reduced by two electrons, now in the dianionic ene-diamide form (note: the label $^{Mes}DAB^{Me}$ is used for both resonance structures of the ligand, but the oxidation state is noted by color in the figures).[12] In this case, the uranium(IV) oxidation state was maintained, relegating the redox chemistry to the ligand rather than uranium. Furthermore, the organic product from C−C coupling, bibenzyl, was also observed spectroscopically.

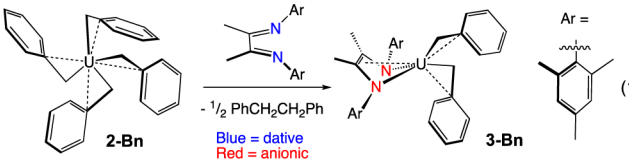

(1)

To complement this study, mechanistic experiments were performed to determine if the reductive elimination proceeded by a concerted (two-electron) or radical (one-electron) pathway. Crossover experiments using **2-Bn** and $U(CD_2C_6D_5)_4$ (**2-Bn-*d*$_{28}$**) confirmed the concerted nature of the reductive elimination,[12] which was in sharp contrast to analogous studies with $Zr(CH_2Ph)_4$ and $Hf(CH_2Ph)_4$.[17−19] For these transition metals, radical chemistry was noted, as benzyl migration to one of the imine carbons of the $^{Mes}DAB^{Me}$ was observed during the

Received: June 12, 2017

DOI: 10.1021/acs.organomet.7b00438
Organometallics XXXX, XXX, XXX−XXX

course of the reaction. Following this, reductive elimination proceeds, with subsequent benzyl migration back to the metal.

Observation of the concerted reductive elimination process was surprising, given that neutral uranium tetrakis(alkyl)s are known to decompose via radical pathways in the absence of ancillary ligands.[20,21] Subsequent to these initial results, we found that inducing reductive elimination from **2-Bn** with an iminoquinone ligand (^{dipp}iq) (^{dipp}iq = 4,6-di-*tert*-butyl-2-[(2,6-diisopropylphenyl)-iminoquinone]), rather than ^{Mes}DAB^{Me}, resulted in a radical process, again confirmed by crossover experiments with **2-Bn-d_{28}**.[22] The dichotomy in reaction mechanism as compared to ^{Mes}DAB^{Me} is attributed to the electrochemical properties of the ligands, as the iminoquinone shows a reversible one-electron wave by cyclic voltammetry, whereas ^{Mes}DAB^{Me} does not.[22]

We established, building on these preliminary results, a general synthetic method based on that for **2-Bn**, which facilitated the synthesis of a substituted uranium tetrabenzyl species, including **2-Bn′** (Bn′ = *p*-^{i}PrBn (**2-*p*-^{i}Pr**), *p*-^{t}BuBn (**2-*p*-^{t}Bu**), *m*-OMeBn (**2-*m*-OMe**), *o*-OMeBn (**2-*o*-OMe**)).[23] These species not only add to the small library of known homoleptic uranium alkyls[12,24−26] but also enable further mechanistic experiments to understand concerted C−C reductive elimination from actinides. Herein, we describe our studies on the influence of electronic effects of benzyl substitution on concerted carbon−carbon reductive elimination from uranium(IV) facilitated by ^{Mes}DAB^{Me}. We combine spectroscopic, magnetic, and kinetic experiments to examine how this important organometallic transformation proceeds for an f-block element.

RESULTS AND DISCUSSION

Synthesis and Characterization of Uranium Compounds. During consideration of the previously synthesized tetrabenzyl−uranium family, [U(*p*-^{i}PrBn)$_4$] (**2-*p*-^{i}Pr**), [U(*p*-^{t}BuBn)$_4$] (**2-*p*-^{t}Bu**), and [U(*m*-OMeBn)$_4$] (**2-*m*-OMe**) were identified as good candidates to complete our mechanistic study, as they were analogous in coordination number and geometry to unsubstituted **2-Bn**. To expand this family, [U(*p*-ClBn)$_4$] (**2-p-Cl**) was targeted for the electron-withdrawing nature of the *p*-chloro substituent. First, the necessary organopotassium reagent, K*p*-ClBn (**1-*p*-Cl**), was synthesized via a modified procedure utilizing Schlosser's base[23,27] by treating a thawing *n*-BuLi/hexane mixture with a thawing slurry of KO^{t}Bu in excess *p*-chlorotoluene. After 5 h of stirring, filtration and workup afforded a light-brown solid. Characterization by ^{1}H NMR spectroscopy (C_6D_6, Figure S22) showed a resonance for the CH_2 protons at 1.11 ppm, while the aryl protons appeared as multiplets in the range of 6.80−7.30 ppm, confirming synthesis of the desired substituted benzylpotassium salt.

Subsequently, synthesis of the homoleptic uranium alkyl, [U(*p*-ClBn)$_4$] , was performed in an analogous manner to the previously reported uranium tetra(alkyl)s by mixing thawing THF solutions of UCl_4 and 4 equivalents of **1-*p*-Cl** (eq 2).[12,23] Following workup, **2-*p*-Cl** was isolated as a dark-brown solid but decomposed after prolonged exposure to THF at room temperature, with *p*-chlorotoluene as the only organic product as observed by ^{1}H NMR spectroscopy; no evidence for the carbon−carbon-coupled product, (1,2-bis(4-chlorophenyl)-ethane), is noted. This is in contrast to **2-Bn**, which produced small amounts of the carbon−carbon-coupled bibenzyl in addition to toluene during decomposition.[12] Optimally, **2-*p*-Cl**

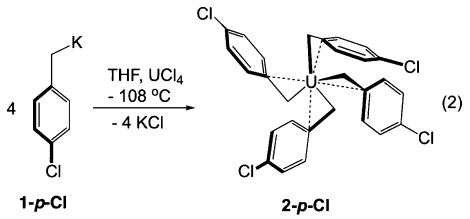

is best stored cold (−35 °C) in the solid state. Analysis of **2-*p*-Cl** by ^{1}H NMR spectroscopy (C_6D_6, Figure S23) shows a resonance for the methylene protons at −72.70 ppm, which is upfield compared to those for **2-*p*-^{i}Pr** and **2-*p*-^{t}Bu**, which are −31.09 to −32.07 ppm, respectively. Such a drastic shift points toward a distinct change in the electronics of the methylene group, which is expected given the relative electron-withdrawing nature of the *p*-chloro group as compared to the electron-donating alkyl substituents.

Magnetic Properties of Uranium Compounds. Given the different electronic properties in this family of homoleptic uranium tetrabenzyl compounds, variable-temperature magnetic-susceptibility measurements were performed for **2-*p*-^{i}Pr**, **2-*p*-^{t}Bu**, **2-*o*-OMe**, **2-*p*-Cl**, and **2-*m*-OMe** to determine the effect, if any, of the electron-donating nature of the benzyl substituent on the magnetic properties. Unfortunately, the parent compound, U(CH_2Ph)$_4$, decomposed too rapidly to include in this study. The measured temperature dependencies of the room-temperature magnetic-susceptibility ($\chi_M T$) products for **2-*p*-^{i}Pr**, **2-*p*-^{t}Bu**, **2-*o*-OMe**, **2-*p*-Cl**, and **2-*m*-OMe** compounds are shown in Figure 1 (data for individual

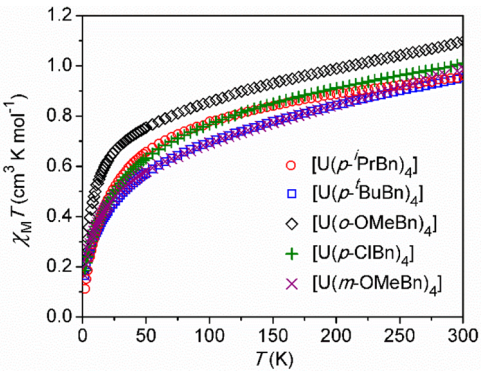

Figure 1. Temperature dependence of magnetic susceptibilities for **2-*p*-^{i}Pr**, **2-*p*-^{t}Bu**, **2-*o*-OMe**, **2-*p*-Cl**, and **2-*m*-OMe**. Data for **2-*p*-^{i}Pr**, **2-*o*-OMe**, and **2-*m*-OMe** were collected at an applied dc field of 5000 Oe, while data for **2-*p*-^{t}Bu** and **2-*p*-Cl** were collected at an applied dc field of 1000 Oe.

complexes are presented as $\chi_M T$ and μ_{eff} values in the Supporting Information, Figures S12−S21), and the tabulated magnetic data for all complexes are presented in Table 1.

At 300 K, the $\chi_M T$ values for **2-*p*-^{i}Pr**, **2-*p*-^{t}Bu**, **2-*o*-OMe**, **2-*p*-Cl**, and **2-*m*-OMe** range from 0.95 to 1.10 cm^{3}Kmol^{-1} (μ_{eff} values range from 2.76 to 2.96). These values slowly decrease upon cooling until approximately 50 K; below this temperature, the $\chi_M T$ values decrease sharply to 0.11−0.26 cm^{3}Kmol^{-1} (μ_{eff} = 0.95−1.23) at 2 K. These magnetic-susceptibility ranges are on the order of those for tetrahedral U(N(SiMe$_3$)$_2$)$_4$ (μ_{eff} = 1.32−2.94)[28] and resemble those reported for tetravalent [U(CH_2^{t}Bu)$_5$]$^-$ (μ_{eff} = 2.36−3.09)[25] and UI(N(SiMe$_3$)$_2$)$_3$ (μ_{eff} = 2.16−3.35).[29] The observed temperature dependencies align with literature precedent for mononuclear tetravalent uranium

DOI: 10.1021/acs.organomet.7b00438
Organometallics XXXX, XXX, XXX−XXX

Table 1. Magnetic Susceptibility and Magnetization Values for 2-*p*-^{i}Pr, 2-*p*-^{t}Bu, 2-*o*-OMe, 2-*p*-Cl, and 2-*m*-OMe

	$\chi_M T$ 300 K ($cm^3 \cdot K \cdot mol^{-1}$)	$\chi_M T$ 2 K ($cm^3 \cdot K \cdot mol^{-1}$)	μ_{eff} 300 K	μ_{eff} 2 K	M 1.8 K, 50 kOe (μ_B)
2-*p*-^{i}Pr	0.96	0.11	2.77	0.95	0.10
2-*p*-^{t}Bu	0.95	0.16	2.76	1.15	0.25
2-*p*-Cl	1.01	0.18	2.84	1.22	0.36
2-*m*-OMe	0.99	0.16	2.81	1.15	0.31
2-*o*-OMe	1.09	0.19	2.96	1.23	0.49

complexes: ground-state singlets show paramagnetic responses at higher temperatures due to population of magnetic excited states. As observed here and previously,[25] complexes containing U−alkyl fragments show distinctive temperature-dependent behavior in that the onset of a sharper downturn in $\chi_M T$ (or μ_{eff}) values occurs at a lower temperature as compared to other U(IV) complexes.

To better understand the magnetic behavior of **2-*p*-^{i}Pr**, **2-*p*-^{t}Bu**, **2-*o*-OMe**, **2-*p*-Cl**, and **2-*m*-OMe**, experiments to study the field dependencies of magnetization were also performed (Figures S2−S11). Although none of the complexes display saturation at 50 kOe, the small magnetization values of 0.10−0.49 μ_B at low temperature (1.8 K) and high field are consistent with ground-state singlets mixed with paramagnetic excited states expected for U(IV) ions, as these values typically remain around 0 μ_B.

Seeking evidence of the synthetic tunability of electronic properties and noting that linear free-energy relationships linking Hammett parameters to spin crossover properties have been described previously,[30] we explored potential trends in magnetization, magnetic susceptibility, and temperature-independent paramagnetism (TIP)[31−34] as a function of substituent donation. **2-*o*-OMe**, which was previously established as an eight-coordinate species arising from ligation to the O atoms,[23] shows the largest susceptibility and magnetization values at all temperatures. This can be attributed to the difference in coordination geometry relative to the rest of the family of compounds and thus precludes further comparison in this study. For the remaining compounds, we observe (Figure 2) a subtle but appreciable correlation between room-temperature magnetic-susceptibility ($\chi_M T$) values and electron-withdrawing ability of the benzyl substituents ($\sigma_{p/m}$). We note that the U−C

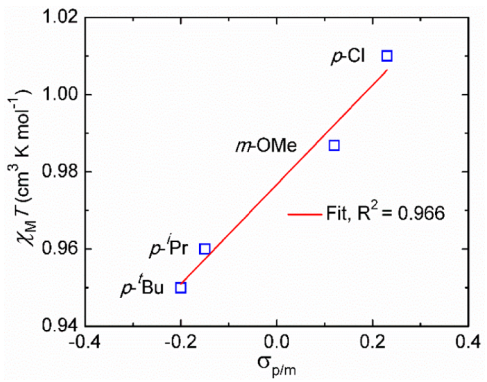

Figure 2. Relationship between the 300 K magnetic-susceptibility values and Hammett parameters for compounds **2-*p*-^{i}Pr**, **2-*p*-^{t}Bu**, **2-*p*-Cl**, and **2-*m*-OMe**. Note that **2-*o*-OMe** was not included in the linear fit due to the difference in inner coordination sphere.

bond distances for these complexes also increase with the increasing electron-withdrawing nature of the substituent, although not with the same linear dependence.[23] The bond-length increase would be expected to weaken σ-overlap between ligands and U frontier orbitals, which would shift magnetic properties toward those associated with a free U(IV) ion (i.e., larger susceptibility values). Further discussion is provided in the Supporting Information. Irrespective of origin, this clear trend could offer a magnetic handle for tracking reactivity.

Reductive Elimination Chemistry. In order to gain insight into the mechanism for reductive elimination, it was first important to confirm that the reductive elimination reaction proceeds in the same manner for **2-*p*-^{i}Pr**, **2-*p*-^{t}Bu**, **2-*m*-OMe**, and **2-*p*-Cl** as for the parent compound, **2-Bn**. In the case of **2-Bn**, addition of the α-diimine ligand, ^{Mes}DAB^{Me}, resulted in extrusion of the carbon−carbon reductive elimination product, bibenzyl, with no observation of toluene, the product of U−C homolytic scission. In the absence of this ligand, only 15% bibenzyl was noted (85% as toluene),[12] indicating the ligand facilitates reductive elimination. Upon addition of ^{Mes}DAB^{Me} to a solution of **2-*p*-^{i}Pr**, **2-*p*-^{t}Bu**, **2-*m*-OMe**, or **2-*p*-Cl**, both the substituted bibenzyl and the ene-diamide uranium(IV) bis(benzyl) complex, (^{Mes}DAB^{Me})U(Bn′)$_2$ (**3-Bn′**; Bn′ = *p*-^{i}PrBn, *p*-^{t}BuBn, *m*-OMeBn, *p*-ClBn) were detected in each case,[12] supporting that the analogous reductive elimination chemistry had occurred.

Evidence of the formation of the substituted bibenzyl was confirmed using ^{1}H NMR spectroscopy by comparison to previously reported data. Positive identification was also possible using mass spectrometry (**2-*p*-^{i}Pr**). In each case, it was evident that the carbon−carbon-coupled product from reductive elimination was formed in significant quantities, with only trace amounts of the substituted toluene noted. For example, in **2-*p*-^{i}Pr**, GC analysis showed ∼85% bibenzyl vs ∼15% toluene formation. However, it should be noted that **3-*p*-^{i}Pr** produces some of the *p*-isopropyl toluene through homolytic scission of the U−C bonds.

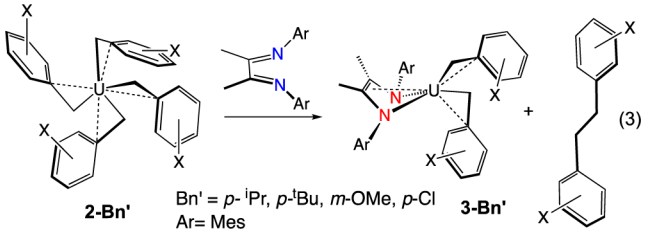

Isolation of the ene-diamide uranium(IV) bis(benzyl) complexes, **3-Bn′**, proved to be difficult, as these species are short-lived in both solution and solid state at room temperature. Nevertheless, isolation of the organometallic products was possible using an independent synthetic route. A representative reaction will be discussed here, that of **2-*p*-^{t}Bu**, since this is the most stable compared to the other members of the family. To analyze the reductive elimination product, a THF solution of **2-*p*-^{t}Bu** was added to a THF solution of ^{Mes}DAB^{Me} while stirring at room temperature. Over the duration of an hour, the dark-brown reaction mixture brightened to brick red. After this time, volatiles were removed in vacuo, and the solid was washed and recrystallized from diethyl ether and pentane.

DOI: 10.1021/acs.organomet.7b00438
Organometallics XXXX, XXX, XXX−XXX

Analysis of the product by ^{1}H NMR spectroscopy (C_6D_6, 23 °C) reveals an asymmetric molecule in solution with 20 paramagnetically shifted and broadened resonances in the range from −80.27 to 82.12 ppm. While structural data could not be obtained due to the inability to grow suitable single X-ray quality crystals for diffraction experiments, support of formation of the **3-Bn′** family was obtained by protonation experiments. Treating **3-Bn′** with 2 equivalents of cracked cyclopentadiene (CpH) generated the substituted toluene and the bis(cyclopentadienyl) uranium ene-diamide product, $Cp_2U(^{Mes}DAB^{Me})$, which has been fully characterized[35] in each case. Further support for the formation of **3-Bn′** derives from the analogous iminoquinone chemistry, where the corresponding radical reductive elimination product, $(^{dipp}ap)_2U(CH_2Ph)_2(THF)_2$ (^{dipp}ap = 4,6-di-*tert*-butyl-2-[(2,6-di-*iso*-propylphenyl)-amidophenolate]), has been crystallographically characterized.[22]

Kinetic Experiments. *Pseudo First-Order Experiments.* In order to probe the effects of the electronics of the benzyl substituent on the reductive elimination, kinetic experiments were conducted in benzene-d_6 at 23 °C and assessed using ^{1}H NMR spectroscopy for **2-Bn**, **2-*p*-^{i}Pr**, **2-*p*-^{t}Bu**, **2-*m*-OMe**, and **2-*p*-Cl** (Figures S24−S31). The reductive elimination reaction is predicted as a second-order reaction, but to accurately quantify a rate law, pseudo first-order conditions were used. By using the uranium alkyl compounds in 10-fold excess and monitoring the loss of the ligand, meaningful kinetics data were obtainable. Ligand monitoring was used to circumvent errors that could be introduced from integration of the paramagnetic uranium species. In light of the entropy of activation data (vide infra), the reductive elimination reaction is associative and thus first order in uranium. The rate constants obtained for each compound are presented in Table 2. The kinetic data show that

Table 2. Rate Constants for Reductive Elimination of 2-Bn,2-*p*-^{i}Pr,2-*p*-^{t}Bu,2-*m*-OMe, and 2-*p*-Cl at 23° C

	reaction rate (10^{-2} k·M^{-1}·sec^{-1})	Hammett parameter ($\sigma_{m/p}$)[a]
2-*p*-^{t}Bu	0.85 (± 0.014)	−0.20
2-*p*-^{i}Pr	1.04 (± 0.097)	−0.15
2-Bn	6.48 (± 0.57)	0
2-*m*-OMe	47.2 (± 4.6)	0.12
2-*p*-Cl	not able to be measured	0.23

[a] σ values taken from Hansch et al.[36]

the rates of the carbon−carbon reductive elimination range from 0.472 (± 0.046) to 0.0085 (± 0.00014), with the compounds containing electron-withdrawing substituents showing substantially faster rates than those featuring electron-donating substituents.

To more accurately correlate the effect of the substituent electron donicity to the rate of reductive elimination, the rate constants were compared to the known Hammett parameter $\sigma_{m/p}$ for the benzyl ring substituents (Table 2). The correlation in the table shows that as the electron-withdrawing effect of the substituent increases, the rate of the reductive elimination reaction also increases: *p*-Cl ≫ *m*-OMe > *p*-H > *p*-^{i}Pr > *p*-^{t}Bu. Reductive elimination of the *p*-chloro derivative is so rapid that it cannot be measured under these standard conditions. This elimination process slows considerably when electron-donating substituents are present on the phenyl ring, including *iso*-propyl and *tert*-butyl substituents. Thus, this system is highly susceptible to the electronic effects of the substitution on the benzyl ligand. This drastic change in rate is well-known for electron-withdrawing substituents and is due to the weakening of the M−C bond that results from the presence of electron-withdrawing substituents that contribute to stronger carbanionic character of the methylene group.

This study marks the first of its kind for carbon−carbon reductive elimination from an actinide center, although the analogous reaction has been studied for group IV metals.[17−19] The radical nature of that reaction precludes a direct comparison here. Rather, the concerted nature of this reaction makes comparison to late transition metals more appropriate. While direct bibenzyl elimination has not been widely studied for transition metals, comparisons can be drawn to systems that involve reductive elimination of substituted phenyls. The observed trend in reductive elimination for uranium(IV) noted here is opposite to that reported for C−C coupling on late transition metals, including $TpNi(CF_3)_2Ar$ (Tp = hydrotris(pyrazolyl)borate; Ar = Ph, *p*-OMePh, *p*-MePh, *p*-BrPh, *m*-CO_2MePh), which forms the aryl-CF_3 product.[37] Instead, the effect of electron-withdrawing substituents noted here for uranium more closely mirrors the C−N coupling of aryl halides with diphenylamine, reported by Buchwald.[38]

To probe the mechanistic details of the reductive elimination reaction, further activation parameters were determined on the basis of the rates listed in Table 1. Due to the sensitive nature of the homoleptic uranium(IV) benzyl family, variable temperature data was collected for **2-*p*-^{i}PrBn**, which is the most stable under the conditions of the experiment, but is also the easiest to synthesize and purify. After performing decomposition control experiments, reductive elimination experiments on **2-*p*-^{i}PrBn** were run from −5 to 25 °C, with ligand disappearance once again monitored by ^{1}H NMR spectroscopy (Figure S32). The concentration of the ligand was plotted vs time in order to calculate the k_{obs} values. These values were used to create an Eyring Plot in order to calculate entropic data (Figure 3). The slope of −3746.8 $\left(-\frac{\Delta H^{\ddagger}}{R}\right)$ gives

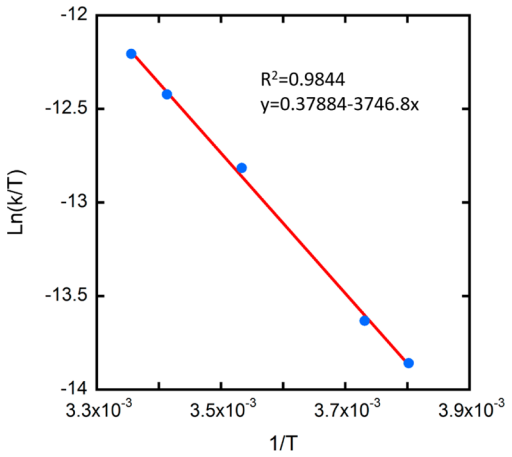

Figure 3. Eyring plot for **2-*p*-^{i}PrBn**.

an enthalpy of activation value of $\Delta H^{\ddagger}$=7.45 ± 0.2 kcal/mol. The y-intercept of 0.3788 $\ln\left(\frac{k_B}{h}\right) + \frac{\Delta S^{\ddagger}}{R}$ gives an entropy value of $\Delta S^{\ddagger}$=−46 ± 0.6 eu. The large magnitude and negative nature of calculated entropy value is indicative of a highly ordered transition state. These parameters, in concert with the previously reported crossover experiment,[12] gives further

DOI: 10.1021/acs.organomet.7b00438
Organometallics XXXX, XXX, XXX−XXX

support that reductive elimination of bibenzyl and its derivatives from **2-Bn**, **2-*p*-^{i}Pr**, **2-*p*-^{t}Bu**, **2-*m*-OMe**, and **2-*p*-Cl** is a concerted process.

On the basis of the experimentally obtained activation parameters as well as the apparent concerted nature of the reaction, a mechanism taking into account these features as well as literature precedent can be proposed (Scheme 1). The initial

Scheme 1. Proposed Mechanism for Carbon−Carbon Reductive Elimination for ^{Mes}DAB^{Me} and U(CH$_2$Ph)$_4$

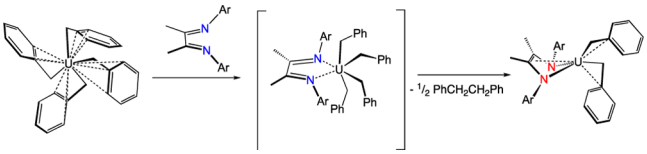

step of the reaction is likely coordination of the neutral ^{Mes}DAB^{Me} ligand to U(CH$_2$Ph)$_4$. While we did not observe (^{Mes}DAB^{Me})U(CH$_2$Ph)$_4$ spectroscopically, its existence is supported by the 1,2-bis(dimethylphosphino)ethane (dmpe) analogue, (dmpe)U(CH$_2$Ph)$_4$, which shows all benzyl groups coordinated in an η^4-fashion in the presence of a bidentate chelator.[12] This ligand association is proposed as the rate-determining step, which is consistent with the negative and large entropy of activation obtained from the kinetic experiments. While the hapticity of the benzyl rings is not known specifically, we hypothesize that their coordination is likely η^2- or greater due to the strong inductive effects noted for electron-withdrawing substituents that are in conjugation.

Following ligand association, it is likely that the steric pressure of ^{Mes}DAB^{Me} drives the carbon−carbon coupling to facilitate the reductive elimination, which would be in direct contrast to stable (dmpe)U(CH$_2$Ph)$_4$, which has a sterically smaller ligand. On the basis of spectroscopic and structural evidence obtained for the product, (^{Mes}DAB^{Me})U(CH$_2$Ph)$_2$, coordinated ^{Mes}DAB^{Me} undergoes reduction by two electrons during this process.

In classical reductive elimination reactions, the two electrons obtained from the reaction revert back to the metal, decreasing the oxidation state by 2. However, since divalent uranium is generally unstable and has only been isolated in specialized ligand environments,[39,40] it is highly unlikely in this case. In accordance with the basic principles of redox-active ligands,[41] the π^* orbitals of ^{Mes}DAB^{Me} are energetically accessible to house these electrons. Previous work from our laboratory has demonstrated electrochemically that the one-electron reduction of ^{Mes}DAB^{Me} to produce [^{Mes}DAB^{Me}]$^{1-}$ is an irreversible process, whereas the two-electron reduction to generate [^{Mes}DAB^{Me}]$^{2-}$ is reversible,[22] thus supporting that concerted two-electron movement is favorable. Furthermore, the lack of reductive elimination noted for (dmpe)U(CH$_2$Ph)$_4$ suggests the role of the empty energetically low-lying orbitals in ^{Mes}DAB^{Me} in facilitating the observed carbon−carbon coupling chemistry. It is highly likely that the uranium acts as a conduit for electron migration from the benzyl groups to the ^{Mes}DAB^{Me} ligand, rather than a sink where the electrons reside for any period of time. In conjunction with the magnetic data, it appears that the rate of reductive elimination increases as the excited-state population is increased on the uranium center. Further studies probing this interesting relationship are underway in our laboratories.

Kinetic experiments in corroboration of the mechanism for any reductive elimination process from actinide centers have not previously been performed. In our particular case, the family of homoleptic uranium tetrabenzyls bearing a variety of substituents are sufficiently stable over a wide temperature range to be able to monitor the reductive elimination reaction spectroscopically. Additionally, it is interesting to note that variation of the electron-donating or electron-withdrawing character of the phenyl ring does not impact the uranium−carbon bond substantially, thus concerted reductive elimination is noted for the entire family. This is important given that nonbenzyl homoleptic uranium alkyl species are seen to decompose over a number of pathways, of which homoleptic U−C scission to produce alkyl radicals is a major contributor.[20,21]

CONCLUSIONS

In summary, we have reported the preparation of a new homoleptic uranium(IV) tetrabenzyl species, U(CH$_2$−*p*-ClBn)$_4$ (**2-*p*-Cl**), that extends our existing family of compounds.[23] Magnetic property measurements of this family reveal a linear free-energy relationship between susceptibility and substituent electronic properties. Significantly, carbon−carbon reductive elimination proceeds readily for this family in a concerted fashion due to the presence of the α-diimine ligand, ^{Mes}DAB^{Me}. The reaction proceeds analogously if electron-donating (^{i}Pr, ^{t}Bu, H) or electron-withdrawing (OMe, Cl) groups are substituted on the phenyl ring, with a drastic rate enhancement noted for electron-withdrawing substituents.

Demonstration of concerted reductive elimination here supports that actinides can perform fundamental organometallic reactions analogously to transition metals. However, there are some stark differences noted for uranium as compared to the d-block metals. First, concerted carbon−carbon bond formation occurs, which is in contrast not only to the group IV derivatives with the ^{Mes}DAB^{Me} ligand[17−19] but also to late first-row transition-metal systems, where bibenzyl elimination is typically a radical process.[42−46] Second, as compared to well studied platinum(IV) systems that are known to undergo C−C reductive elimination with aryl groups, using electron-withdrawing groups on the uranium-benzyl rings promotes an increased rate of reductive elimination, rather than a slower one. With the unique features of this system in mind, future studies will be focused toward expanding the scope and mechanistic understanding of the reductive elimination reaction to heteroatoms and other alkyl substituents.

EXPERIMENTAL SECTION

General Considerations. All air- and moisture-sensitive manipulations were performed using standard Schlenk techniques or in an MBraun inert atmosphere drybox with an atmosphere of purified nitrogen. The MBraun drybox was equipped with a cold well designed for freezing samples in liquid nitrogen as well as two −35 °C freezers for cooling samples and crystallizations. Solvents for sensitive manipulations were dried and deoxygenated using literature procedures with a Seca solvent-purification system.[47] Benzene-d_6 and toluene-d_8 were purchased from Cambridge Isotope Laboratories, dried with molecular sieves and sodium, and degassed by three freeze−pump−thaw cycles. THF-d_8 was purchased from Cambridge Isotope Laboratories and used as received. Potassium *t*-butoxide and *n*-butyllithium (2.5 M in hexanes) were purchased from Sigma-Aldrich and used as received. *p*-Chlorotoluene was purchased from Sigma-Aldrich and distilled from CaH$_2$ prior to use. Uranium tetrachloride,[48]

DOI: 10.1021/acs.organomet.7b00438
Organometallics XXXX, XXX, XXX−XXX

^{Mes}DAB^{Me},[49] **2-Bn**,[12] **2-*p*-^{i}Pr**, **2-*p*-^{t}Bu**, **2-*o*-OMe**, **2-*m*-OMe**[23] were prepared according to literature procedures.

^{1}H NMR and ^{13}C NMR spectra were recorded on a Varian Inova 300 spectrometer operating at 299.992 and 75.424 MHz, respectively. ^{1}H NMR spectra for kinetic experiments were recorded on a Varian Inova 600 spectrometer operating at 599.967 MHz. All chemical shifts are reported relative to the peak for $SiMe_4$, using ^{1}H (residual) chemical shifts of the solvent as a secondary standard. The spectra for paramagnetic molecules were obtained by using an acquisition time of 0.5 s, thus the peak widths reported have an error of ±2 Hz. For paramagnetic molecules, the ^{1}H NMR data are reported with the chemical shift, followed by the peak width at half height, the integration value and, where possible, the peak assignment.

Magnetic-susceptibility data were collected using a Quantum Design MPMS XL SQUID magnetometer. All sample preparations were performed inside a dinitrogen-filled glovebox (MBRAUN Labmaster 130). Powdered microcrystalline samples were loaded into polyethylene bags and sealed in the glovebox, inserted into a straw and transported to the magnetometer under dinitrogen. Ferromagnetic impurities were checked through a variable field analysis (0 to 10 kOe) of the magnetization at 100 K: curvature in the M vs H plot between 0 and ∼2000 Oe (Figures S2−S6) indicates the presence of ferromagnetic impurities. When this behavior was observed, susceptibility data were collected at magnetic fields where the field dependence is linear (usually 5000 Oe). Magnetic-susceptibility data were collected at temperatures ranging from 2 to 300 K. Susceptibility data reproducibility was assessed through measurements on two different batches for compound **1**, which showed consistency at all temperatures, with a maximum difference of 0.03 $cm^3 \cdot K \cdot mol^{-1}$ at 300 K. Magnetization measurements were collected at 1.8 K while varying the applied field up to 50 kOe (Figures S7−S11). Data were corrected for the diamagnetic contributions of the sample holder and bag by subtracting empty containers; corrections for the sample were calculated from Pascal's constants.[50]

*Synthesis of Kp-ClBn (**1-p-ClBn**).* A modified procedure for organopotassium reagents, reported by Schlosser,[23,27] was used to generate the series of organopotassium reagents. A 250 mL round-bottom flask was charged with 2.00 g (17.8 mmol) of KO^{t}Bu and excess *p*-chlorotoluene (100 mL). The slurry was cooled in the cold well for ∼20 min or until frozen. While stirring, cold (−35 °C), *n*-butyllithium (2.5 M in hexanes, 7.12 mL, 17.8 mmol) was added to the thawing slurry, producing an immediate color change to light brown. The solution was allowed to warm to room temperature for 5 h at which point the mixture darkened to deep brown. The brown solid was collected using a fritted funnel and washed with a continuous stream of pentane totaling approximately ∼200 mL to remove any remaining substituted toluene and LiO^{t}Bu. The solid was dried on the vacuum line and identified as K*p*-ClBn (**1-*p*Cl**). Quantitative yields were obtained. ^{1}H NMR (THF-d_8, 25 °C): δ = 1.11 (s, 2H, CH_2), 6.80−7.30 (m, 4H, C*H*).

Synthesis of U(p-Cl-Bn)$_4$(2-p-Cl). A 20 mL vial was charged with 0.050 g of green UCl_4 and 2 mL of THF. A second vial was charged with 4 equivalents of light-brown **1-*p*Cl** and 2 mL of THF. Each vial was frozen in the cold well to −108 °C and mixed upon thawing. The mixture immediately turned dark brown whereupon THF was removed in vacuo. The brown residue was triturated in diethyl ether and filtered to remove KCl. Drying the filtrate produced **2-*p*-Cl** as a brown solid (55%). Due to the sensitivity and instability of the compound, reliable elemental analysis could not be obtained. ^{1}H NMR (C_6D_6, 25 °C): δ = −72.64 (s, 8H, CH_2), 1.58 (s, 8H, *m*-C*H*), 93.24 (s, 8H, o−C*H*).

Synthesis of ^{Mes}DAB^{Me}U(p-^{t}BuBn)$_2$. A 20 mL scintillation vial was charged with 0.050 g of **2-*p*-^{t}Bu** in ∼5 mL of THF. A second vial was charged with 1 equivalent of ^{Mes}DAB^{Me} in ∼5 mL of THF. The two solutions were mixed at room temperature while stirring. Over an hour, the dark-brown solution brightens slightly to red brown. After an additional hour, the volatiles were removed under vacuum, and the isolated brown powder was recrystallized from diethyl ether and pentane. ^{1}H NMR (C_6D_6, 25 °C): δ = −80.27 (1H), −52.28 (2H), −27.16(3H), −22.12 (2H), −12.32 (9H), −10.69 (2H), −8.74 (1H), −8.20 (1H), −7.35 (9H), −4.93 (1H), −1.10 (3H), 1.07 (6H), 9.77 (2H), 15.05 (3H), 18.43(1H), 23.63 (1H) 37.14 (1H), 59.82 (1H), 60.04 (3H), 82.12 (6H).

General Experimental Kinetics. Stock solutions of ferrocene (0.08 M), ^{Mes}DAB^{Me} (0.08 M), and homoleptic uranium(IV) tetra-alkyl compound (0.1 M) in benzene-d_6 were prepared. Four samples of the uranium compounds were diluted to different concentrations ranging from 0.02 to 0.07 M. Ferrocene stock solution (20 μL) was added to each uranium sample as a standard. Four different solutions of known concentrations were added to four different screw-cap NMR tubes that were then sealed with tape. Four syringes (50 μL) were filled with 20 μL of ^{Mes}DAB^{Me} and inserted into rubber septa to limit atmospheric exposure. Once removed from the glovebox, the NMR tubes were placed in liquid nitrogen to prevent decomposition between experiments. Kinetics experiments were run in a 600 MHz Varian NMR spectrometer at a constant temperature as an array experiment. Four scans were performed per run with a 1 s delay between runs. The runs covered a 50 k sweep width, a 7 s delay time, and a 0.5 s acquisition time. Before placement into the instrument, the samples were thawed in a room-temperature water bath, and then, the ligand was injected and thoroughly mixed. Data were analyzed via MestReNova and visualized with KaliedaGraph software.

■ ASSOCIATED CONTENT

Supporting Information

The Supporting Information is available free of charge on the ACS Publications website at DOI: 10.1021/acs.organomet.7b00438.

Additional experimental procedures, magnetic data, and spectroscopic data (PDF)

■ AUTHOR INFORMATION

Corresponding Author

*E-mail: sbart@purdue.edu.

ORCID

Mahdi M. Abu-Omar: 0000-0002-4412-1985

Matthew P. Shores: 0000-0002-9751-0490

Suzanne C. Bart: 0000-0002-8918-9051

Author Contributions

The manuscript was written through contributions of all authors.

Notes

The authors declare no competing financial interest.

■ ACKNOWLEDGMENTS

We acknowledge the National Science Foundation (CAREER grant to S.C.B., CHE-1149875) for funding. M.P.S. and R.F.H. thank NSF (CHE-1363274) for support of magnetometry measurements at Colorado State University. Prof. David McMillin is acknowledged for helpful discussions.

■ REFERENCES

(1) Racowski, J. M.; Dick, A. R.; Sanford, M. S. *J. Am. Chem. Soc.* **2009**, *131*, 10974−10983.

(2) Ghosh, R.; Emge, T. J.; Krogh-Jespersen, K.; Goldman, A. S. *J. Am. Chem. Soc.* **2008**, *130*, 11317−11327.

(3) Madison, B. L.; Thyme, S. B.; Keene, S.; Williams, B. S. *J. Am. Chem. Soc.* **2007**, *129*, 9538−9539.

(4) Gatard, S.; Celenligil-Cetin, R.; Guo, C.; Foxman, B. M.; Ozerov, O. V. *J. Am. Chem. Soc.* **2006**, *128*, 2808−2809.

(5) Culkin, D. A.; Hartwig, J. F. *Organometallics* **2004**, *23*, 3398−3416.

(6) Williams, B. S.; Goldberg, K. I. *J. Am. Chem. Soc.* **2001**, *123*, 2576−2587.

DOI: 10.1021/acs.organomet.7b00438
Organometallics XXXX, XXX, XXX−XXX

(7) Goldberg, K. I.; Yan, J. Y.; Winter, E. L. *J. Am. Chem. Soc.* **1994**, *116*, 1573−1574.
(8) Ghosh, R.; Zhang, X.; Achord, P.; Emge, T. J.; Krogh-Jespersen, K.; Goldman, A. S. *J. Am. Chem. Soc.* **2007**, *129*, 853−866.
(9) Ananikov, V. P.; Musaev, D. G.; Morokuma, K. *J. Am. Chem. Soc.* **2002**, *124*, 2839−2852.
(10) Crumpton, D. M.; Goldberg, K. I. *J. Am. Chem. Soc.* **2000**, *122*, 962−963.
(11) Johnson, S. A.; Bart, S. C. *Dalton Trans.* **2015**, *44*, 7710−7726.
(12) Kraft, S. J.; Fanwick, P. E.; Bart, S. C. *J. Am. Chem. Soc.* **2012**, *134*, 6160−6168.
(13) Zucchini, U.; Giannini, U.; Albizzati, E.; D'Angelo, R. *J. Chem. Soc. D* **1969**, 1174−1175.
(14) Felten, J. J.; Anderson, W. P. *J. Organomet. Chem.* **1972**, *36*, 87−92.
(15) Ballard, D. G.; van Lienden, P. W. *Makromol. Chem.* **1972**, *154*, 177−190.
(16) Koehler, E.; Brueser, W.; Thiele, K.-H. *J. Organomet. Chem.* **1974**, *76*, 235−240.
(17) Froese, R. D. J.; Jazdzewski, B. A.; Klosin, J.; Kuhlman, R. L.; Theriault, C. N.; Welsh, D. M.; Abboud, K. A. *Organometallics* **2011**, *30*, 251−262.
(18) Figueroa, R.; Froese, R. D.; He, Y.; Klosin, J.; Theriault, C. N.; Abboud, K. A. *Organometallics* **2011**, *30*, 1695−1709.
(19) De Waele, P.; Jazdzewski, B. A.; Klosin, J.; Murray, R. E.; Theriault, C. N.; Vosejpka, P. C.; Petersen, J. L. *Organometallics* **2007**, *26*, 3896−3899.
(20) Marks, T. J.; Seyam, A. M. *J. Organomet. Chem.* **1974**, *67*, 61−66.
(21) Marks, T. J.; Seyam, A. M. *J. Am. Chem. Soc.* **1972**, *94*, 6545−6546.
(22) Matson, E. M.; Franke, S. M.; Anderson, N. H.; Cook, T. D.; Fanwick, P. E.; Bart, S. C. *Organometallics* **2014**, *33*, 1964−1971.
(23) Johnson, S. A.; Kiernicki, J. J.; Fanwick, P. E.; Bart, S. C. *Organometallics* **2015**, *34*, 2889−2895.
(24) Fortier, S.; Walensky, J. R.; Wu, G.; Hayton, T. W. *J. Am. Chem. Soc.* **2011**, *133*, 11732−11743.
(25) Fortier, S.; Melot, B. C.; Wu, G.; Hayton, T. W. *J. Am. Chem. Soc.* **2009**, *131*, 15512−15521.
(26) Van der Sluys, W. G.; Burns, C. J.; Sattelberger, A. P. *Organometallics* **1989**, *8*, 855−857.
(27) Schlosser, M.; Hartmann, J. *Angew. Chem., Int. Ed. Engl.* **1973**, *12*, 508−509.
(28) Lewis, A. J.; Williams, U. J.; Carroll, P. J.; Schelter, E. J. *Inorg. Chem.* **2013**, *52*, 7326−7328.
(29) Fortier, S.; Brown, J. L.; Kaltsoyannis, N.; Wu, G.; Hayton, T. W. *Inorg. Chem.* **2012**, *51*, 1625−1633.
(30) Lin, H.-J.; Siretanu, D.; Dickie, D. A.; Subedi, D.; Scepaniak, J. J.; Mitcov, D.; Clérac, R.; Smith, J. M. *J. Am. Chem. Soc.* **2014**, *136*, 13326−13332.
(31) Newell, B. S.; Rappé, A. K.; Shores, M. P. *Inorg. Chem.* **2010**, *49*, 1595−1606.
(32) Almond, P. M.; Deakin, L.; Porter, M. J.; Mar, A.; Albrecht-Schmitt, T. E. *Chem. Mater.* **2000**, *12*, 3208−3213.
(33) Kiplinger, J. L.; Pool, J. A.; Schelter, E. J.; Thompson, J. D.; Scott, B. L.; Morris, D. E. *Angew. Chem., Int. Ed.* **2006**, *45*, 2036−2041.
(34) Schelter, E. J.; Morris, D. E.; Scott, B. L.; Thompson, J. D.; Kiplinger, J. L. *Inorg. Chem.* **2007**, *46*, 5528−5536.
(35) Kraft, S. J.; Williams, U. J.; Daly, S. R.; Schelter, E. J.; Kozimor, S. A.; Boland, K. S.; Kikkawa, J. M.; Forrest, W. P.; Christensen, C. N.; Schwarz, D. E.; Fanwick, P. E.; Clark, D. L.; Conradson, S. D.; Bart, S. C. *Inorg. Chem.* **2011**, *50*, 9838−9848.
(36) Hansch, C.; Leo, A.; Taft, R. W. *Chem. Rev.* **1991**, *91*, 165−195.
(37) Bour, J. R.; Camasso, N. M.; Sanford, M. S. *J. Am. Chem. Soc.* **2015**, *137*, 8034−8037.
(38) Arrechea, P. L.; Buchwald, S. L. *J. Am. Chem. Soc.* **2016**, *138*, 12486−12493.
(39) MacDonald, M. R.; Fieser, M. E.; Bates, J. E.; Ziller, J. W.; Furche, F.; Evans, W. J. *J. Am. Chem. Soc.* **2013**, *135*, 13310−13313.
(40) La Pierre, H. S.; Scheurer, A.; Heinemann, F. W.; Hieringer, W.; Meyer, K. *Angew. Chem., Int. Ed.* **2014**, *53*, 7158−7162.
(41) Chirik, P. J. *Inorg. Chem.* **2011**, *50*, 9737−9740.
(42) van der Meer, M.; Rechkemmer, Y.; Peremykin, I.; Hohloch, S.; van Slageren, J.; Sarkar, B. *Chem. Commun.* **2014**, *50*, 11104−11106.
(43) Osako, T.; Karlin, K. D.; Itoh, S. *Inorg. Chem.* **2005**, *44*, 410−415.
(44) Shey, J.; McGinley, C. M.; McCauley, K. M.; Dearth, A. S.; Young, B. T.; van der Donk, W. A. *J. Org. Chem.* **2002**, *67*, 837−846.
(45) Jacobson, R. R.; Tyeklár, Z.; Karlin, K. D. *Inorg. Chim. Acta* **1991**, *181*, 111−118.
(46) Carmona, E.; Paneque, M.; Poveda, M. L. *Polyhedron* **1989**, *8*, 285−291.
(47) Pangborn, A. B.; Giardello, M. A.; Grubbs, R. H.; Rosen, R. K.; Timmers, F. J. *Organometallics* **1996**, *15*, 1518−1520.
(48) Kiplinger, J. L.; Morris, D. E.; Scott, B. L.; Burns, C. J. *Organometallics* **2002**, *21*, 5978−5982.
(49) Zhong, H. A.; Labinger, J. A.; Bercaw, J. E. *J. Am. Chem. Soc.* **2002**, *124*, 1378−1399.
(50) Bain, G. A.; Berry, J. F. *J. Chem. Educ.* **2008**, *85*, 532−536.

DOI: 10.1021/acs.organomet.7b00438
Organometallics XXXX, XXX, XXX−XXX